THE JOURNAL OF PHYSICAL CHEMISTRY A

ARTICLE

pubs.acs.org/JPCA

Electronic Energy Migration in Solid versus Liquid Host Matrices for Concentrated Perylenediimide Dye Solutions

Kathryn A. Colby and Christopher J. Bardeen*

Department of Chemistry, University of California, Riverside, Riverside, California 92521, United States

ABSTRACT: In this paper, we continue our evaluation of Forster-type theories of exciton diffusion in disordered environments. The perylenediimide dye Lumogen Red is used as a donor molecule in two different liquids, $CHCl_3$ and dimethylformamide, and the energy transfer to the acceptor molecule Rhodamine 700 is measured using time-resolved fluorescence decays. The exciton motion is measured over Lumogen Red concentrations ranging from 1×10^{-4} to 5×10^{-2} M, and the results are compared to previous results for exciton diffusion in a solid polymer. Depending on the theoretical approach used to analyze the data, we find that the energy migration in the liquids is a factor of 2−3 faster than in the solid polymer, even after taking molecular translation into account. Measurements for a Lumogen Red concentration of 10 mM in the different host environments yield diffusion constants ranging from 2.2 to 3.1 nm^2/ns in the liquids, as compared to 1.1−1.2 nm^2/ns in solid poly(methyl methacrylate) (PMMA). The results in the liquids are in good agreement with theoretical predictions and numerical simulations of previous workers, while the results in solid PMMA are 2−3 times slower. This discrepancy is discussed in the context of the rapid energetic averaging present in the liquid environments but absent in the solid matrix, where unfavorable configurations and low energy trapping sites are frozen in by the static disorder.

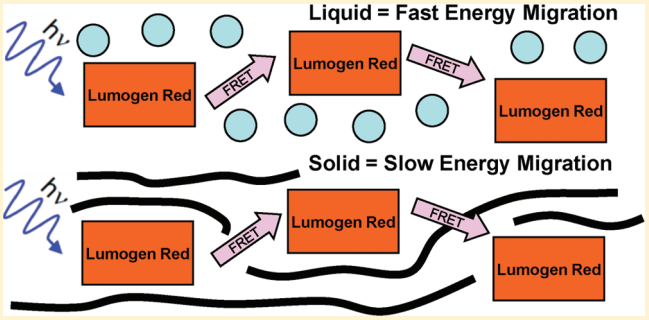

1. INTRODUCTION

The efficiency of electronic devices composed of conjugated organic molecules can depend sensitively on the rate of exciton diffusion through the material. For example, organic photovoltaic materials rely on exciton diffusion to charge separation interfaces to transform photon energy into an electrochemical potential. The overall solar energy conversion efficiency of an organic solar cell depends directly on the exciton diffusion length (L_D) in organic semiconductors.[1−4] Thus, there is a need to understand quantitatively how chemical properties influence L_D so that improved materials can be designed for higher efficiency organic solar cells. Most organic photovoltaic materials are based on semiconducting polymers and tend to be amorphous solids. The physical picture is that these disordered solids are composed of molecular chromphores (e.g., polymer segments) that couple to each other through weak electronic interactions. Electronic energy transfer (EET) between segments is thought to proceed through an incoherent hopping mechanism. Forster and subsequent workers derived the following analytical expression for the three-dimensional exciton diffusion constant D_{EET}[5−9]

$$D_{EET} = \eta \left(\frac{4\pi C}{3}\right)^{4/3} \frac{R_0^6}{\tau_{fl}} \tag{1}$$

where C is the chromophore number density and τ_{fl} is the fluorescence lifetime of the donor in the absence of EET. The prefactor η can be thought of as a correction factor that takes the molecular details of the system into account and ranges from 0.32 to 0.56 depending on the theoretical method used to estimate it. The energy transfer rate between molecules is given by

$$k_{FRET} = \frac{1}{\tau_{FRET}} = \frac{1}{\tau_{fl}} \left(\frac{R_0}{R}\right)^6 \tag{2a}$$

where R is the separation between molecules and the critical Forster radius R_0 is given by

$$R_0^6 = \frac{9000 \ln(10) \phi_{fl} \kappa^2}{128 \pi^5 N_A n^4} \int_0^\infty \varepsilon(\nu) f(\nu) \frac{d\nu}{\nu^4} \tag{2b}$$

where n is the index of refraction; ϕ_{fl} is the fluorescence quantum yield; κ is an orientation factor; N_A is Avagodro's number; $\varepsilon(\nu)$ is the absorption spectrum of the acceptor; and $f(\nu)$ is the donor's fluorescence spectrum whose integral has been normalized to 1. Most measurements estimate L_D to be on the order of 10 nm in amorphous solids,[10−12] so it is important to study energy migration in well-characterized model systems and evaluate whether eq 1 can provide a basis for designing organic semiconductors with enhanced exciton motion and superior photovoltaic properties.

Received: March 21, 2011
Revised: May 5, 2011
Published: June 07, 2011

We recently used time-resolved fluorescence anisotropy and quenching decays to study whether eq 1 provides an acceptable description of EET in a system that is both amorphous and also safely in the regime of incoherent Forster-type energy transfer.[13] In that work, hereafter referred to as Paper I, it was necessary to use a dye−polymer system where the chromophore concentration could be varied over several orders of magnitude without aggregation. The perylenediimide dye Lumogen Red (LR) serves as an excellent model system for validating theories for exciton diffusion since it was designed to avoid aggregation[14−16] and is extremely photostable.[17,18] For LR doped into PMMA, we found that the anisotropy decay, which reflects the initial energy transfer event from the initially excited LR molecule to one of its neighbors, could be quantitatively described by the Gouchancour−Anderson−Fayer (GAF) theory of EET in a static disordered system.[6,19] However, when fluorescence quenching experiments were used to assess the longer range motion of the exciton, we found that the GAF theory version of eq 1 significantly overestimated the diffusion rate, as did other theoretical approaches. For a LR concentration of 10 mM in PMMA, we obtained experimental values for D_{EET} ranging from 0.32 to 1.20 nm^2/ns, depending on the method used to analyze the experimental data. In contrast, various theoretical approaches predicted values ranging from 3.7 to 8.6 nm^2/ns.

Recently, Lochbrunner and co-workers used steady-state spectroscopic methods to study energy migration in a closely related system, LR in poly(methyl methacrylate) (PMMA) with the dye Oxazine 1 as an acceptor.[20] The concentration range they studied was higher than in this work, but they found that their experimental D_{EET} values were only a factor of 2 smaller than the theoretical values. This apparent discrepancy may be taken as further evidence that the absolute value of D_{EET} can depend sensitively on the experimental approach (different acceptor molecules, steady-state fluorescence spectra versus time-resolved decays) used to extract the absolute value of D_{EET}. In this paper, we concentrate on how changing the environment affects the relative values of D_{EET}. To complement our earlier PMMA studies, we repeat the LR/R700 concentration-dependent fluorescence quenching experiments in liquid environments, where dynamic fluctuations provide a qualitatively different type of disorder. The use of the LR/R700 system in both liquids and solid PMMA allows us to focus on the effects of changing the environment since chemical factors like molecular volume,[7,21] specific donor−acceptor interactions,[22−24] and breakdowns in the point-dipole approximation[25−29] should all be similar in the different environments, allowing relative comparisons to be made. The novel aspect of the current work is that it quantitatively shows, using a single donor−acceptor system, how moving from a solid to a liquid host changes the energy migration rate. In liquids, we find the measured energy diffusion is more rapid than in solid PMMA. Experiments on two chemically distinct liquids, chloroform ($CHCl_3$) and dimethylformamide (DMF), yield similar results. The fact that theory appears to quantitatively describe energy migration in liquids but not in a solid suggests that some aspect of the theory breaks down in the solid. We suggest that different types of energetic disorder are at the origin of the discrepancy. In the liquids, rapid averaging over different configurations prevents the exciton from becoming trapped at a stationary low energy site. In a truly inhomogeneously broadened solid, on the other hand, an exciton can become trapped at a low energy site that remains constant for the remainder of its lifetime. Our results are consistent with the idea that static disorder in amorphous solids plays an important role in determining exciton diffusion rates.

2. EXPERIMENTAL SECTION

Lumogen Red (LR) was donated by BASF and purified via silica gel column chromatography with a 90%:10%-by-volume mixture of CH_2Cl_2 and hexanes. H^1 NMR and LC-mass spectra confirmed the purity to be 99% and indicated that the carboxylic bisimide[30] and *N*-methyl-2-pyrrolidone[31] impurities commonly found in LR were successfully removed. PMMA (average molecular weight = 80 000, Aldrich), Rhodamine 700 (Exciton), and all solvents were used as received. Liquid solutions were made by combining the appropriate amounts of dye and measured volumes of either chloroform ($CHCl_3$) or dimethylformamide (DMF).

For the liquid samples, we made custom spectroscopic cells with path lengths of 1−2 μm to ensure peak optical densities below 0.2 and avoid self-absorption artifacts. These cells were made using reverse-phase photolithography to deposit a metal barrier onto a glass microscope slide. Photoresist was deposited onto the glass slide, exposed to patterned UV radiation, and then dissolved where we wanted to place the side walls of the cell. A thin layer of titanium (∼200 Å) followed by a thicker layer of gold (1 μm) was deposited onto the developed areas of the slide with a Temescal BJD-1800 E-beam evaporator. Finally, the remaining photoresist inside the sample area of the cell was dissolved away, leaving an open area surrounded by a 1−2 μm high wall of evaporated gold. A DekTak 8 surface profilometer was used to confirm the height of the deposited metal film. Spring-loaded binder clips were used to seal a second glass slide on top of the gold film and prevent evaporation of solvent during measurements.

Steady state absorption spectra were acquired using a Cary 50 spectrometer. All steady state fluorescence measurements were taken on a Horiba Jovin-Spex-3 fluorimeter with front-face detection and 550 nm excitation. For fluorescence measurements, the sample absorption was checked to ensure that all films and liquid solutions possessed peak optical densities of less than 0.2 to avoid self-absorption effects. Time-resolved experiments were performed with a regeneratively amplified Ti-Sapphire laser operating at a 40 kHz repetition rate with its fundamental wavelength at 800 nm. The 800 nm beam was focused onto a sapphire plate from which a continuum was generated. A 10 nm bandwidth interference filter was used to select a portion of the continuum centered at 550 nm for fluorescence excitation. Laser powers ranged from 0.5 to 1.5 μW to prevent saturation effects in the streak camera. The diameter of the laser spot incident on the sample was ∼130 μm. All samples were excited using front face excitation and detection, and the fluorescence was passed through a polarizer set at 54.7° (the magic angle) to extract decays free from molecular rotational effects. After passing through a Schott glass OG570 cutoff filter, the fluorescence was detected using a Hamamatsu C4337 streak camera with 2 nm spectral resolution and 15 ps time resolution. To isolate the LR fluorescence, the signals were integrated between 570 and 620 nm to prevent contamination of the LR signal by R700 fluorescence.

3. RESULTS AND DISCUSSION

1. Theoretical Basis for Extraction of Energy Migration Observables. In this section, we briefly review the method used to estimate D_{EET} used in our previous paper[13] and note some

modifications for the liquid experiments. We posit a general form for the fluorescence decay in the presence of quenchers as[7,32−35]

$$I_D(t) = I_D(0)\exp\left[-\frac{t}{\tau_{fl}} - At - A't - B\sqrt{t}\right] \quad (3)$$

$$A = 4\pi D_{EET}\sigma_F C_A \quad (4a)$$

$$A' = 4\pi D_{trans}\sigma_F C_A \quad (4b)$$

$$B = \frac{4}{3}\pi R_{DA}^3 C_A\sqrt{\pi k_{fl}} \quad (4c)$$

where τ_{fl} is the fluorescent lifetime for the donor (LR) in the absence of quenchers; D_{EET} is the diffusion of the excitation due to energy transfer; D_{trans} is the sum of the translational diffusion coefficients of the donor and acceptor molecules; σ_F is the quenching radius; C_A is the acceptor concentration; and R_{DA} is the donor−acceptor Forster radius. A is the decay term due to energy migration; A' results from molecular translation; and B represents a single-step energy transfer from donor to acceptor. In this expression, A depends on the concentration of the donor molecule, defined as C_D, through its dependence on D_{EET}. Note that in solid matrices $D_{trans} = 0$. Since the parameter of interest is the energy migration rate of the donor, the A term within the donor's fluorescence signal needs to be isolated. This is accomplished by dividing the fluorescence signal at large values of C_D, where energy migration is present, by the signal for low C_D where energy migration is negligible.[36] Experimentally, the fluorescence decay becomes slower as $C_D = C_{LR}$ decreases and then reaches a constant value after 0.1 mM. The 0.1 and 0.01 mM signals from both the solid and liquid matrices overlapped. Therefore, in agreement with what has been found by others,[37] the $C_{LR} = 0.1$ mM samples were used as the baseline corresponding to the case where no energy migration was present. When the fluorescence decay at high C_{LR} is divided by that at low C_{LR}, all the concentration-independent terms should cancel out, leaving only the decay component due to the A term which reflects energy migration

$$\frac{I(t)[\text{high } C_{LR}]}{I(t)[low C_{LR}]} = \frac{\exp[-k_{fl}t - At - A't - B\sqrt{t}]}{\exp[-k_{fl}t - A't - B\sqrt{t}]} = \exp[-At] \quad (5)$$

From eq 4a it would appear that extracting D_{EET} from A should be a simple matter of dividing by the quantity $4\pi\sigma_F C_A$. In general, however, σ_F is not a constant but depends on D_{EET}. This dependence arises from the fact that as the donor intermolecular distance decreases excitons travel faster so that the donor−donor transfer rate becomes competitive with the donor−acceptor quenching rate, and the exciton quenching becomes less effective. In this paper, we will consider two limits for σ_F to extract quantitative values for D_{EET} from the measured A values. The first limit consists of assuming that

$$D_{EET} = kC_D^{\alpha}R_{DD}^6 \quad (6)$$

Note that if eq 1 is valid, $\alpha = 4/3$ and $k = \eta/(\tau_{fl})((4\pi)/3)^{4/3}$. In this approach, we take α, the power-law dependence of D_{EET} on C_D, to be an experimentally determined variable, but assume that $\sigma_F = R_{DA}$. If we substitute eq 6 into eq 4, we obtain the following expression for A

$$A = 4\pi k C_D^{\alpha}R_{DD}^6 R_{DA}C_A \quad (7)$$

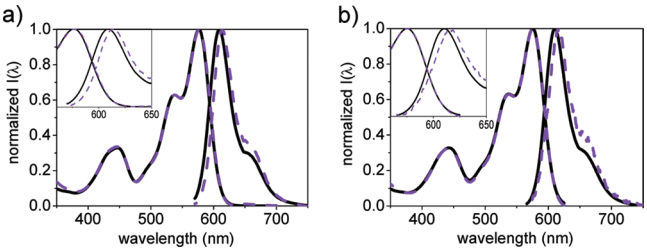

Figure 1. Spectral shifting of LR steady state spectra in (a) $CHCl_3$ and (b) DMF with increasing LR concentration: 10^{-4} M LR (—), and 50 mM LR (purple - - -).

An alternate approach involves using an approximate expression to describe how σ_F depends on D_{EET} and thus C_{LR} as given in eq 8[7]

$$\sigma_F \cong R_{DA}\frac{\Gamma(0.75)}{2\Gamma(1.75)}\left(\frac{k_S R_{DA}^2}{D_{EET}}\right)^{1/4} = 0.676\left(\frac{R_{DA}^6}{D_{EET}\tau_{fl}}\right)^{1/4} \quad (8)$$

If we now assume that eq 1 provides an accurate description of D_{EET}, we can use eqs 1, 4a, and 8 to derive an analytical expression for the value of A, which explicitly depends on the scaling factor η

$$A = \eta^{3/4}\frac{35.58R_{DA}^{3/2}R_{DD}^{9/2}}{\tau_{fl}}C_A C_D \quad (9)$$

All parameters in eq 9 are known except η, so a plot of A versus C_D should yield η, and then eq 1 can be used to calculate D_{EET}.

We close with a brief discussion of using eqs 3−9 to extract D_{EET} from the fluorescence quenching decays. As discussed at length in Paper I, there exist different methods for extracting the diffusion constant from the fluorescence decay data, and we found that applying these different theories to our LR/R700 data in PMMA resulted in experimental D_{EET} values that varied by roughly a factor of 4. Thus, the values we extract for D_{EET} should be viewed as most useful for making relative comparisons between environments, rather than as absolute determinations of the actual D_{EET} values.

2. Energy Migration in Liquids. We wanted to examine whether there is a difference between hosts with static disorder, as found in amorphous PMMA, and those with dynamic disorder, namely, liquid solvents. We chose two solvents where both donor and acceptor molecules had good solubility. The fact that R700 is a salt while LR is nonpolar eliminated several classes of solvents, such as alcohols and alkanes, from consideration, but we found both molecules were highly soluble in DMF and $CHCl_3$. We first characterized the steady state spectroscopy of LR in $CHCl_3$ and DMF to obtain an accurate estimate of the Forster radius. Figure 1 shows that the LR fluorescence spectrum shifts toward the red in DMF and $CHCl_3$. This is in contrast to PMMA, where the absorption shifts toward the blue while the emission remains stationary. The shifts in wavelength reflect interactions between LR molecules that shift the energy levels of the absorbing and emitting states. Since LR is expected to be more polarizable than any of the host matrices, increasing its concentration would be expected to increase the overall polarizability of the medium, increasing the Stokes shift and decreasing the spectral overlap between absorption and emission and thus decreasing R_{DD} as well. The curious thing is that the increased polarity at higher C_{LR} values appears to stabilize the ground state LR in PMMA (causing a blue shift in the absorption) and the excited state in the liquids (causing a red-shift in the fluorescence).

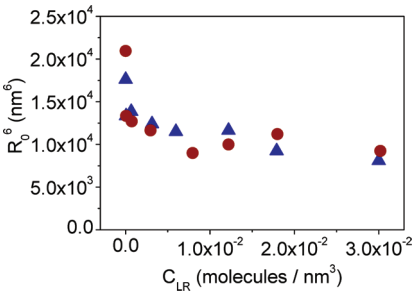

Figure 2. Decrease in R_{DD}^6 with increasing LR concentration in $CHCl_3$ (●) and DMF (▲).

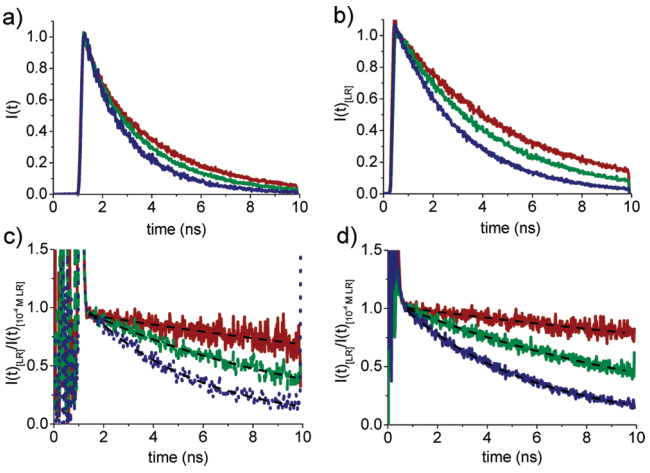

Figure 3. Raw (a,b) and divided fluorescence decays (c,d) for 10 mM (red), 25 mM (green), and 50 mM (blue) LR in $CHCl_3$ (a,c) and DMF (b,d). The value for A^{-1} for each sample was extracted by fitting the decays with a single exponential: 28 ns (red), 9.5 ns (green), and 4.6 ns (blue) for $CHCl_3$-based samples (c) and 37 ns (red), 12 ns (green), and 5 ns (blue) for DMF-based samples (d).

The reason for the different shifting of the spectra behavior of LR in the two liquids as opposed to PMMA is unknown at this time. In all three host materials a reduction of the spectral overlap is the end result of such concentration-dependent shifts and, along with it, a reduction in R_{DD}. This reduction of the Forester radius R_0 that depends on C_{LR} must be taken into account to accurately determine how A (and thus D_{EET}) depends on C_{LR}. Figure 2 shows this decrease in R_{DD}^6 versus C_{LR} for the two solvents in this current study, similar to what was observed for PMMA in Paper I.

We can calculate the appropriate Forster radii for LR→LR (D→D) and LR→R700 (D→A) energy transfer using the steady state data and eqs 2 and 3. The quantum yield of LR was taken to be 0.96 in the solvents and 0.88 in PMMA.[38] The κ^2 orientational term was set to 0.476 for solid PMMA and 0.667 for the liquids.[39] The refractive indexes were set to 1.49 in PMMA, 1.45 in $CHCl_3$, and 1.43 in DMF. The Forster radii were found to be $R_0 = R_{DD}$ = 4.36 nm, 4.46 nm, and 4.77 nm for C_{LR} = 10 mM in $CHCl_3$, DMF, and PMMA, respectively. The fluorescence lifetime τ_{fl} was measured to be 5.7 ns in PMMA and 6.2 ns in the liquids.[13,38] R_{DA} was taken to be 5.85 nm for all cases.

Once the concentration dependence of R_{DD}^6 has been determined, we can analyze the fluorescence decays to extract D_{EET}. The experimental analysis outlined in Section 1 and performed previously for PMMA was repeated in $CHCl_3$ and DMF. The LR concentration was varied from 0.01 to 50 mM, while the R700 concentration C_{R700} was fixed at 0.5 mM. Note that a lower quencher concentration was used in the liquids than in PMMA (where C_{R700} = 2.0 mM) because the fluorescence quenching was significantly stronger in the liquids. Figures 3a and 3c show the raw signals, showing how the fluorescence decay rates increase as C_{LR} increases. The value for A was extracted as described in Section 1 by dividing the raw fluorescence signals at higher values of C_{LR} by the C_{LR} = 0.1 mM fluorescence decay, which left the ratio decays shown in Figures 3b and 3d. These decays were then fit to single exponential decays to extract the A values.

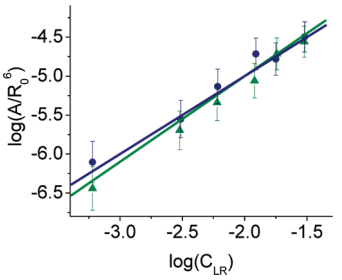

Figure 4. Log−log plot of the decay constant A, scaled by the concentration-dependent Forster radius, versus C_{LR} with the acceptor R700 concentration set to 0.5 mM. The lines represent the linear least-squares fits with slope = α = 1.0 ± 0.2 for the data in in $CHCl_3$ (●) and α = 1.1 ± 0.2 in DMF.

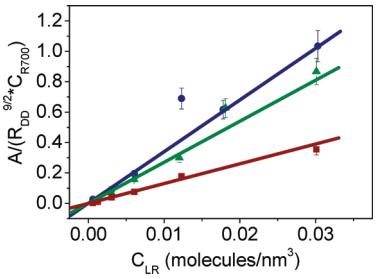

Figure 5. Plot of the diffusional quenching constant A term, scaled by the concentration-dependent Forster radius, versus C_{LR}. Linear least-squares fits to the data yield slopes of 34 for $CHCl_3$ (●), 27 for DMF (▲), and 13 for PMMA (■). Using eq 9, the values of the scaling factor η in eq 1 are found to be 0.23 in DMF, 0.31 in $CHCl_3$, and 0.08 in PMMA.

The first question we want to address is how A depends on C_{LR}. Equation 7 allows the power-law dependence α to be a free parameter, while eq 9 predicts a linear dependence on both C_{LR} and C_{R700}. In Figure 4, we adopt the assumption of eq 7 and look at how the quantity A/R_{DD}^6 varies with C_{LR}. The log−log plots in Figure 4 yield slopes of 1.0 ± 0.2 for $CHCl_3$ and 1.1 ± 0.2 for DMF, confirming the linear dependence of A on C_{LR} predicted by eq 9. Note that for this treatment we take the dependence of R_{DD} on C_{LR} into account by dividing by a factor of R_{DD}^6, as suggested by eq 7. In paper I, we found that dividing by either R_{DD}^6 (which assumes that σ_F is constant) or by $R_{DD}^{9/2}$ (as suggested by eq 9) did not affect the value of α. This was found to also be the case for the liquids. In paper I, the log−log plot of A versus C_{LR} in PMMA yielded a slope of 1.2 ± 0.2. The small difference in α values observed in the liquids relative to solid PMMA is consistent with the prediction that in a solid environment D_{EET} (and thus A) should exhibit a stronger dependence on C_{LR} than in liquids.[7] The

dx.doi.org/10.1021/jp202654v |J. Phys. Chem. A 2011, 115, 7574–7581

Table 1. D and L_D for 10 mM LR in $CHCl_3$, DMF, and PMMA Based on Various Theories and Experimental Analysis of Fluorescence Quenching Data[a]

	$CHCl_3$		DMF		PMMA	
method for estimating D	D (nm^2/ns)	L_D (nm)	D (nm^2/ns)	L_D (nm)	D (nm^2/ns)	L_D (nm)
theory, eq1, $\eta = 0.56$ (ref 7)	4.6	13.1	5.3	14	8.6	17.1
theory, eq1, $\eta = 0.43$ (ref 6)	3.5	11.4	4.0	12.3	6.6	15.0
theory, eq1, $\eta = 0.32$ (ref 9)	2.6	9.9	3.0	10.6	4.9	12.9
experimental, eqs 4a and 6, $\sigma_F = R_{DA}$	3.1	10.7	2.2	9.1	1.1	5.5
experimental, eqs 1 and 9, $\sigma_F \approx D$	2.6	9.7	2.2	9.0	1.2	6.4

[a] L_D is calculated using $(6D\tau_{fl})^{1/2}$ and assuming a fluorescence lifetime (τ_{fl}) of 5.70 ns in PMMA and 6.2 ns in the solvents in the absence of acceptors. R_{DD} for C_{LR} = 10 mM is 4.77 nm in PMMA, 4.46 nm in DMF, and 4.36 nm in $CHCl_3$.

fact that both solid and liquid media exhibit an A dependence on C_{LR} similar to that predicted theoretically is encouraging.

Since the data in Figure 4 are consistent with the $\alpha = 1.0$ dependence of A on C_{LR} predicted by eq 9, we decided to use both eqs 7 and 9 to extract values of D_{EET} from the experimentally measured A values. First, using eq 7, we find that $A = 11.4C_{LR}^{1.0}$ for $CHCl_3$ and $A = 13.5C_{LR}^{1.1}$ for DMF with $C_{R700} = 0.5$ mM, while $A = 44.6C_{LR}^{1.2}$ in PMMA with $C_{R700} = 2$ mM. Given these empirical relations, and assuming $\sigma_F = R_{DA}$, we can use eqs 6 and 7 to calculate D_{EET}. For $C_{LR} = 10$ mM, we find values for D_{EET} of 3.1 and 2.2 nm^2/ns for $CHCl_3$ and DMF, respectively, while the same type of analysis for PMMA yields a value of $D_{EET} = 1.1$ nm^2/ns. This value is slightly larger than the value of 0.89 nm^2/ns reported for the same approach in paper I, due to the use of $\alpha = 1.2$ instead of $\alpha = 1.24$ in the earlier work. In this paper, we have rounded the α value to be consistent with the number of significant figures used in the other calculations.

Alternatively, we can use eq 9 to extract a value for η and then calculate D_{EET} using eq 1. In Figure 5 we plot the dependence of the experimental quantity $A/(R_{DD}^{9/2}C_{R700})$ versus C_{LR} for all three systems. From the slope of these lines, we can extract the η values in accordance with eq 9. The data in liquid $CHCl_3$ and DMF can be quantitatively described using values of $\eta = 0.31$ and $\eta = 0.23$, respectively, while in PMMA we find $\eta = 0.08$, as in paper I. The η values in the liquids are reasonably close to the value of $\eta = 0.32$ predicted by Haan−Zwanzig theory[9] and are a factor of 3−4 larger than that found for PMMA. These values of η can be plugged into eq 1 to generate a second set of values for D_{EET}: 2.6 nm^2/ns in $CHCl_3$, 2.2 nm^2/ns in DMF, and 1.2 nm^2/ns in PMMA. Table 1 summarizes the experimental values of D_{EET} obtained in this work for $C_{LR} = 10$ mM in the three different media, along with the predictions of three different theoretical approaches. Note that although we have not reported explicit experimental error values in Table 1 they are on the order of 10−20%, errors arising from the assumptions in the models being at least as large as the experimental errors. The agreement between the two methods for DMF is probably fortuitous, given the error range of the experiment. While we have concentrated on analyzing the $C_{LR} = 10$ mM data, it is important to note that eqs 1, 6, and 9 permit us to estimate D_{EET} for any value of C_{LR}. For example, values of C_{LR} as high as 100 mM are achievable in room-temperature liquid solutions,[14,20] and using the value $D_{EET} = 2.6$ nm^2/ns for $C_{LR} = 10$ mM in $CHCl_3$, according to eq 1, this higher value of C_{LR} would enhance D_{EET} by a factor of $10^{3/4}$, resulting in $D_{EET} = 56$ nm^2/ns and a diffusion length L_D on the order of 45 nm. This large diffusion length is approaching the dimensions of typical thin organic photovoltaic devices, albeit in liquid form.

The agreement between experiment and theory for the liquids is remarkably good, considering the approximations used to derive eqs 4−9. Our results are also consistent with experimental results and numerical simulations done by Miller and co-workers that indicated $\eta = 0.20 \pm 0.03$ for disodium fluorescein in ethanol.[40,41] It should be emphasized that within the framework of our analysis the increased D_{EET} for the liquids is not due to simple translational motion of the molecules. The D_{trans} contribution should be independent of C_{LR} and, like the B term in eq 3, should be divided out when the high and low C_{LR} decays are divided using eq 5. If the translational motion and energy migration are not completely decoupled as assumed, then it is possible for D_{EET} to be enhanced beyond the theoretical values. The basic idea is that fluctuations in the intermolecular separation R, allowed in a liquid but not in a solid, can provide transient opportunities for EET that would not otherwise occur. This phenomenon has been explored theoretically[7,42] and becomes important at very high donor concentrations. Experiments by Joshi et al. appear to suggest that this effect can enhance D_{EET} up to 2 orders of magnitude beyond that predicted by eq 1.[43] However, our extracted D_{EET} values are quite close to what is predicted by eq 1, and there is no experimental indication of a large enhancement in D_{EET} by translational motion. The dynamic nature of liquids can affect other parameters, in addition to R, that determine the energy transfer rate given by eqs 2a and 2b. Rotational diffusion can permit the κ^2 orientational factor to fluctuate. In principle, this difference is taken into account through the κ^2 factors that differ in the solid (0.476) and liquids (0.667). The success of the basic theory in predicting D_{EET} in liquids suggests that it does a reasonably good job of taking into account the effects of disorder in R and κ^2. The mystery is why it fails to describe the EET dynamics in the solid PMMA matrix, where Forster-type theories correctly predicted the qualitative dependence of D_{EET} on C_{LR}, but overestimates the absolute values by roughly a factor of 5−7.

One aspect of disordered environments that the theory does not explicitly address is the fact that different local configurations can shift the energies of neighboring molecules and cause the spectral overlap term in eq 2b to vary. Hole-burning and photon echo experiments have shown that spectral diffusion in liquids permits chromophores to sample the entire absorption line shape within a nanosecond or less, going from high to low energy configurations many times within their excited state lifetime.[44−48] Just as rapid rotational diffusion averages over different molecular orientations, spectral diffusion can average over different energy configurations in liquids. This rapid averaging of configurations has been invoked previously to explain enhanced triplet diffusion in liquids.[49,50] This effect would explain why a theory that does not take energetic

disorder explicitly into account can still accurately describe energy migration in a liquid. While we have not yet performed such nonlinear optical experiments on LR in the various matrices considered in this paper, it seems likely that the spectral diffusion observed in other types of dyes would be present in LR as well. Dyes in a solid polymer, on the other hand, are truly inhomogeneously broadened with chromophores that can never fully explore the available energy landscape.[51−55] Many earlier studies have implicated static disorder as a culprit responsible for dispersive transport and lower-than-expected exciton diffusion rates in solids.[56−62] Our experimental results suggest that for the LR/R700 system in PMMA this reduces the effective diffusion constant by a factor of 2−4. In general, static disorder will lead to anomalous diffusion and can only be taken into account using more sophisticated numerical models whose implementation is beyond the scope of this paper.[63−66] However, recent theoretical results suggest that a knowledge of the distribution of energies may be sufficient to modify eq 1 so that it can still give a quantitative description of exciton diffusion in disordered solids.[67] One way to test this concept is to vary the amount of dynamic versus static energetic disorder (analogous to homogeneous and inhomogeneous broadening) in a controlled manner, for example by changing temperature or the solvent viscosity. Since DMF is more viscous than $CHCl_3$, the faster exciton diffusion in $CHCl_3$ provides preliminary evidence that such factors can play a role. Ideally, parallel measurements of the energetic disorder (using four-wave mixing experiments like the photon echo) and exciton diffusion (using fluorescence quenching or the transient grating) as a function of environment could be used to establish a quantitative connection between these two quantities.

4. CONCLUSIONS

The results presented here represent a continuation of our study of how electronic energy travels through disordered systems. In paper I, we found that for LR embedded in PMMA energy migration falls short of the predictions based on eq 1, with an experimental $\eta = 0.08$ instead of the theoretically predicted value of $\eta = 0.32-0.56$. When exciton migration in liquids is measured, we find that $\eta = 0.23-0.31$, close to the value of $\eta = 0.32$ predicted by Haan−Zwanzig theory. While this agreement may be fortuitous, our results clearly demonstrate that exciton diffusion is more rapid in fluid environments, even after the molecular center-of-mass translational diffusion is taken into account. One possible explanation for this phenomenon is the ability of liquid environments to "wash out" energetic configurations that can trap the excitation on relatively short time scales. If we picture the exciton traversing an energy landscape defined by different molecular-level conformations of the matrix, then the peaks and valleys provide opportunities for the exciton to become trapped. In a solid, these peaks and valleys are stationary, and the exciton remains trapped during its lifetime. In a liquid, these peaks and valleys are rapidly shifting like waves on the sea, allowing the exciton to escape during its lifetime. In the drive to increase solar energy conversion efficiencies, engineering disorder in organic semiconductors may provide one avenue to enhance exciton diffusion lengths and improve photocurrent yields.

AUTHOR INFORMATION

Corresponding Author

*E-mail: christopher.bardeen@ucr.edu. Phone: 951-827-2723. Fax: 951-827-4713.

ACKNOWLEDGMENT

This research was supported by the National Science Foundation, grant DMR-0907310. The short path length spectroscopic cells were fabricated in the UCR Center for Nanoscale Science & Engineering with the aid of Dexter Humphrey.

REFERENCES

(1) Gregg, B. A. Excitonic solar cells. *J. Phys. Chem. B* **2003**, *107*, 4688–4698.

(2) Guenes, S.; Neugebauer, H.; Sariciftci, N. S. Conjugated polymer-based organic solar cells. *Chem. Rev.* **2007**, *107*, 1324–1338.

(3) Yang, F.; Forrest, S. R. Photocurrent generation in nanostructured organic solar cells. *ACS Nano* **2008**, *2*, 1022–1032.

(4) Walker, A. B. Multiscale modeling of charge and energy transport in organic light-emitting diodes and photovoltaics. *Proc. IEEE* **2009**, *97*, 1587–1596.

(5) Forster, T. *Ann. Phys.* **1948**, *2*, 55.

(6) Gochanour, C. R.; Andersen, H. C.; Fayer, M. D. Electronic excited state transport in solution. *J. Chem. Phys.* **1979**, *70*, 4254–4271.

(7) Jang, S.; Shin, K. J.; Lee, S. Effects of excitation migration and translational diffusion in the luminescence quenching dynamics. *J. Chem. Phys.* **1995**, *102*, 815–827.

(8) Loring, R. F.; Andersen, H. C.; Fayer, M. D. Electronic excited state transport and trapping in solution. *J. Chem. Phys.* **1982**, *76*, 2015–2027.

(9) Haan, S. W.; Zwanzig, R. Forster migration of electronic excitation between randomly distributed molecules. *J. Chem. Phys.* **1978**, *68*, 1879–1883.

(10) Scully, S. R.; McGehee, M. D. Effects of optical interference and energy transfer on exciton diffusion length measurements in organic semiconductors. *J. Appl. Phys.* **2006**, *100*, 034907/1–034907/5.

(11) Shaw, P. E.; Ruseckas, A.; Samuel, I. D. W. Exciton diffusion measurements in poly(3-hexylthiophene). *Adv. Mater.* **2008**, *20*, 3516–3520.

(12) Lunt, R. R.; Giebink, N. C.; Belak, A. A.; Benziger, J. B.; Forrest, S. R. Exciton diffusion lengths of organic semiconductor thin films measured by spectrally resolved photoluminescence quenching. *J. Appl. Phys.* **2009**, *105*, 053711/1–053711/7.

(13) Colby, K. A.; Burdett, J. J.; Frisbee, R. F.; Zhu, L.; Dillon, R. J.; Bardeen, C. J. Electronic energy migration on different timescales: concentration dependence of the time-resolved anisotropy and fluorescence quenching of Lumogen Red in poly(methyl methacrylate). *J. Phys. Chem. A* **2010**, *114*, 3471–3482.

(14) Al-Kaysi, R. O.; Ahn, T. S.; Muller, A. M.; Bardeen, C. J. The photophysical properties of chromophores at high (100 mM and above) concentrations in polymers and as neat solids. *Phys. Chem. Chem. Phys.* **2006**, *8*, 3453–3459.

(15) Seybold, G.; Wagenblast, G. New perylene and violanthrone dyestuffs for fluorescent collectors. *Dyes Pigm.* **1989**, *11*, 303–317.

(16) Langhals, H.; Ismael, R.; Yuruk, O. Persistent fluorescence of perylene dyes by steric inhibition of aggregation. *Tetrahedron* **2000**, *56*, 5435–5441.

(17) Sark, W. G. J. H. M. v.; Barnham, K. W. J.; Sloof, L. H.; Chatten, A. J.; Buchtemann, A.; Meyer, A.; Mccormack, S. J.; Koole, R.; Farrell, D. J.; Bose, R.; Bende, E. E.; Burgers, A. R.; Budel, T.; Quilitz, J.; Kennedy, M.; Meyer, T.; Donega, C. D. M.; Meijeriink, A.; Vanmaekelbergh, D. Luminescent solar concentrators -- a review of recent results. *Opt. Express* **2008**, *16*, 21773–21792.

(18) Tanaka, N.; Barashkov, N.; Heath, J.; Sisk, W. Photodegradation of polymer-dispersed perylene di-imide dyes. *Appl. Opt.* **2006**, *45*, 3846–3851.

(19) Gochanour, C. R.; Fayer, M. D. Electronic excited-state transport in random systems. Time-resolved fluorescence depolarization measurements. *J. Phys. Chem.* **1981**, *85*, 1989–1994.

(20) Fennel, F.; Lochbrunner, S. Long distance energy transfer in a polymer matrix doped with a perylene dye. *Phys. Chem. Chem. Phys.* **2011**, *13*, 3527–3533.

(21) Rangelowa-Jankowska, S.; Kulak, L.; Bojarski, P. Nonradiative long range energy transfer in donor-acceptor systems with excluded volume. *Chem. Phys. Lett.* **2008**, *460*, 306–310.
(22) Barbosa-Garcia, O.; Struck, C. W. Monte Carlo treatment of the nonradiative energy transfer process for nonrandom placements of dopants in solids. *J. Chem. Phys.* **1994**, *100*, 4554–4568.
(23) Kaschke, M.; Vogler, K. Picosecond study of energy transfer. Deviations from Forster theory -- evidence fo an inhomogeneous spatial distribution of molecules. *Chem. Phys.* **1986**, *102*, 229–240.
(24) Wang, Z.; Holden, D. A.; McCourt, F. R. W. Monte Carlo simulation of singlet energy migration and trapping in nonrandom chromophore distributions generated by photoraction in glassy polymer matrices. *Macromolecules* **1991**, *24*, 893–900.
(25) Beenken, W. J. D.; Pullerits, T. Excitonic coupling in polythiophenes: comparison of different calculation methods. *J. Chem. Phys.* **2004**, *120*, 2490–2495.
(26) Curutchet, C.; Mennucci, B.; Scholes, G. D.; Beljonne, D. Does Forster predict the rate of electronic energy transfer for a model dyad at low temperature?. *J. Phys. Chem. B* **2008**, *112*, 3759–3766.
(27) Ortiz, W.; Krueger, B. P.; Kleiman, V. D.; Krause, J. L.; Roitberg, A. E. Energy transfer in the nanostar: the role of coulombic coupling and dynamics. *J. Phys. Chem. B* **2005**, *109*, 11512–11519.
(28) Scholes, G. D. Long-range resonance energy transfer in molecular systems. *Annu. Rev. Phys. Chem.* **2003**, *54*, 57–87.
(29) Wong, K. F.; Bagchi, B.; Rossky, P. J. Distance and orientational dependence of excitation transfer rates in conjugated systems: beyond the Forster theory. *J. Phys. Chem. A* **2004**, *108*, 5752–5763.
(30) Clendinen, C.; Sisk, W.; Nishikiori, H.; Tanaka, N.; Fuji, T. Energy transfer and photodegradation of perylene red with DTTC and HITC acceptor dyes in PMMA. *Dyes Pigm.* **2008**, *77*, 92–97.
(31) Garcia-Moreno, I.; Costela, A.; Pintado-Sierra, M.; Martin, V.; Sastre, R. Enahnced laser action of perylene red-doped polymeric materials. *Opt. Express* **2009**, *17*, 12777–12784.
(32) Powell, R. C.; Soos, Z. G. Singlet exciton energy transfer in organic solids. *J. Lumin.* **1975**, *11*, 1–45.
(33) Gosele, U.; Hauser, M.; Klein, U. K. A.; Frey, R. Diffusion and long-range energy transfer. *Chem. Phys. Lett.* **1975**, *34*, 519–522.
(34) Pandey, K. K. Electronic excitation transport, diffusion and trapping. *Chem. Phys.* **1992**, *165*, 123–134.
(35) Pandey, K. K.; Pant, T. C. Diffusion-modulated energy transfer. *Chem. Phys. Lett.* **1990**, *170*, 244–252.
(36) Renschler, C. L.; Faulkner, L. R. Design of an antenna system for the collection of singlet excitation energy. Exciton diffusion among concentrated 9,10-diphenylanthracene centers in polystyrene. *J. Am. Chem. Soc.* **1982**, *104*, 3315–3320.
(37) Miller, R. J. D.; Pierre, M.; Fayer, M. D. Electronic excited state transport and trapping in disordered systems: picosecond fluorescence mixing, transient grating, and probe pulse experiments. *J. Chem. Phys.* **1983**, *78*, 5138–5146.
(38) Ahn, T. S.; Al-Kaysi, R. O.; Muller, A. M.; Wentz, K. M.; Bardeen, C. J. Self-absorption corrections for solid-state photoluminescence quantum yields obtained from integrating sphere measurements. *Rev. Sci. Instrum.* **2007**, *78*, 086105/1–086105/3.
(39) Baumann, J.; Fayer, M. D. Excitation transfer in disordered two-dimensional and anisotropic three-dimensional systems: effects of spatial geometry on time-resolved observables. *J. Chem. Phys.* **1986**, *85*, 4087–4107.
(40) Gomez-Jahn, L.; Kasinski, J.; Miller, R. J. D. Spatial properties of electronic excited state energy transport in three-dimensional disordered systems: picosecond transient grating studies. *Chem. Phys. Lett.* **1986**, *125*, 500–506.
(41) Reiger, P. T.; Palese, S. P.; Miller, R. J. D. On the Forster model: computational and ultrafast studies of electronic energy transport. *Chem. Phys.* **1997**, *221*, 85–102.
(42) Sienicki, K.; Mattice, W. L. Forward and reverse energy transfer in the presence of energy migration and correlations. *J. Chem. Phys.* **1989**, *90*, 6187–6192.
(43) Joshi, H. C.; Mishra, H.; Tripathi, H. B.; Pant, T. C. Role of diffusion in excitation energy transfer: a time-resolved study. *J. Lumin.* **2000**, *90*, 17–25.
(44) Cruz, C. H. B.; Fork, R. L.; Knox, W. H.; Shank, C. V. Spectral hole buring in large molecules probed with 10 fs optical pulses. *Chem. Phys. Lett.* **1986**, *132*, 341–344.
(45) Kang, T. J.; Yu, J.; Berg, M. Limitations on measuring solvent motion with ultrafast transient hole burning. *J. Chem. Phys.* **1991**, *94*, 2413–2424.
(46) Boeij, W. P. d.; Pshenichnikov, M. S.; Wiersma, D. A. System-bath correlation function probed by conventional and time-gated stimulated photon echo. *J. Phys. Chem.* **1996**, *100*, 11806–11823.
(47) Passino, S. A.; Nagasawa, Y.; Joo, T.; Fleming, G. R. Three-pulse echo peak shift studies of polar solvation dynamics. *J. Phys. Chem. A* **1997**, *101*, 725–731.
(48) Scholes, G. D.; Larsen, D. S.; Fleming, G. R.; Rumbles, G.; Burn, P. L. Origin of line broadening in the electronic absorption spectra of conjugated polymers: Three-pulse-echo studies of MEH-PPV in toluene. *Phys. Rev. B* **2000**, *61*, 13670–13678.
(49) Holzman, P.; Jarnagin, R. C. Triplet energy migration in pure fluids. *J. Chem. Phys.* **1969**, *51*, 2251–2253.
(50) Pautmeier, L.; Ries, B.; Richert, R.; Bassler, H. Disorder-enhanced triplet exciton diffusion in condensed aromatic systems. *Chem. Phys. Lett.* **1988**, *143*, 459–462.
(51) Narasimhan, L. R.; Bai, Y. S.; Dugan, M. A.; Fayer, M. D. Observation of fast time scale spectral diffusion in a low temperature glass: comparison of picosecond photon and stimulated echoes. *Chem. Phys. Lett.* **1991**, *176*, 335–342.
(52) Bardeen, C. J.; Cerullo, G.; Shank, C. V. Temperature-dependent electronic dephasing of molecules in polymers in the range 30 to 300 K. *Chem. Phys. Lett.* **1997**, *280*, 127–133.
(53) Nagasawa, Y.; Passino, S. A.; Joo, T.; Fleming, G. R. Temperature dependence of optical dephasing in an organic polymer glass (PMMA) from 300 to 30 K. *J. Chem. Phys.* **1997**, *106*, 4840–4852.
(54) Zilker, S. J.; Kador, L.; Friebel, J.; Vainer, Y. G.; Kolchenko, M. A.; Personov, R. I. Comparison of photon echo, hole burning and single molecule spectroscopy data on low temperature dynamics of organic amorphous solids. *J. Chem. Phys.* **1998**, *109*, 6780–6790.
(55) Nagasawa, Y.; Seike, K.; Muromoto, T.; Okada, T. Two-dimensional analysis of integrated three-pulse photon echo signals of nile blue doped in PMMA. *J. Phys. Chem. A* **2003**, *107*, 2431–2441.
(56) Stein, A. D.; Peterson, K. A.; Fayer, M. D. Dispersive excitation transport at elevated temperatures (50−298 K): Experiments and theory. *J. Chem. Phys.* **1990**, *92*, 5622–5635.
(57) Meskers, S. C. J.; Hubner, J.; Oestreich, M.; Bassler, H. Dispersive relaxation dynamics of photoexcitations in a polyfluorene film involving energy transfer: experiment and Monte Carlo simulations. *J. Phys. Chem. B* **2001**, *105*, 9139–9149.
(58) Mollay, B.; Lemmer, U.; Kersting, R.; Mahrt, R. F.; Kurz, H.; Kauffmann, H. F.; Bassler, H. Dynamics of singlet excitons in conjugated polymers: Poly(phenylenevinylene) and poly(phenylphenylvinylene). *Phys. Rev. B* **1994**, *50*, 10769–10779.
(59) Gaab, K. M.; Bardeen, C. J. Wavelength and temperature dependence of the femtosecond pump-probe anisotropies in the conjugated polymer MEH-PPV: Implications for energy transfer dynamics. *J. Phys. Chem. B* **2004**, *108*, 4619–4626.
(60) Gaab, K. M.; Bardeen, C. J. Anomalous exciton diffusion in the conjugated polymer MEH-PPV measured using a three-pulse pump-dump-probe anisotropy experiment. *J. Phys. Chem. A* **2004**, *108*, 10801–10806.
(61) Madigan, C.; Bulovic, V. Modeling of exciton diffusion in amorphous organic thin films. *Phys. Rev. Lett.* **2006**, *96*, 046404/1–046404/4.
(62) Arkhipov, V. I.; Emelianova, E. V.; Bassler, H. On the role of spectral diffusion of excitons in sensitized photoconduction in conjugated polymers. *Chem. Phys. Lett.* **2004**, *383*, 166–170.
(63) Katsuura, K. Exciton migration in one-dimensional molecular random lattices. *J. Chem. Phys.* **1964**, *40*, 3527–3530.

(64) Schonherr, G.; Eiermann, R.; Bassler, H.; Silver, M. Dispersive exciton transport in a hopping system with guassian energy distribution. *Chem. Phys.* **1980**, *52*, 287–298.

(65) Poulsen, L.; Jazdzyk, M.; Communal, J. E.; Sancho-Garcia, J. C.; Mura, A.; Bongiovanni, G.; Beljonne, D.; Cornil, J.; Hanack, M.; Egelhaaf, H. J.; Gierschner, J. , Three-dimensional energy transport in highly luminescent host-guest crystals: a quantitative experimental and theoretical study. *J. Am. Chem. Soc.* **2007**, *129*, 8585–8593.

(66) Ahn, T. S.; Wright, N.; Bardeen, C. J. The effects of orientational and energetic disorder on Forster energy migration along a one-dimensional lattice. *Chem. Phys. Lett.* **2007**, *446*, 43–48.

(67) Athansopoulos, S.; Emelianova, E. V.; Walker, A. B.; Beljonne, D. Exciton diffusion in energetically disordered organic materials. *Phys. Rev. B* **2009**, *80*, 195209/1–195209/7.